IEEE Access
Multidisciplinary ⋮ Rapid Review ⋮ Open Access Journal

Received December 13, 2021, accepted January 18, 2022, date of publication January 27, 2022, date of current version February 10, 2022.

Digital Object Identifier 10.1109/ACCESS.2022.3146885

Reconfigurable Intelligent Surface-Assisted HAPS Relaying Communication Networks for Multiusers Under AF Protocol: A Performance Analysis

KEHINDE OLUWASESAN ODEYEMI[1], PIUS ADEWALE OWOLAWI[2], (Member, IEEE), AND OLADAYO OLUFEMI OLAKANMI[1]

[1]Department of Electrical and Electronic Engineering, Faculty of Technology, University of Ibadan, Ibadan 200005, Nigeria
[2]Department of Computer Systems Engineering, Tshwane University of Technology, Pretoria 0001, South Africa

Corresponding author: Kehinde Oluwasesan Odeyemi (ko.odeyemi@ui.edu.ng)

ABSTRACT This research paper studies the performance analysis of a reconfigurable intelligent surface (RIS)-assisted high altitude platform station (HAPS) relaying communication network for multiple ground users. Owing to transmission blockage between the source and the destination, the source transmits its information to the HAPS via the RIS where the HAPS acts as an amplify-and-forward (AF) relay node for sending the source information to ground users. To characterize the transmission links, the channels between the source-RIS-HAPS are assumed to follow approximate generalized-K fading distribution while the links between the HAPS and multiple ground users experience Shadowing-Rician fading distribution. Since HAPS employs AF relaying scheme, the closed-form expressions of the cumulative distribution function (CDF) and probability density function (PDF) of the system end-to-end signal-to-noise ratio (SNR) are derived by exploiting the Meijer's G and Fox's H functions. Based on these expressions, the analytical expressions of the system outage probability, average bit error rate (BER) and average capacity are obtained to examine the system performance. Moreover, the asymptotic expressions are obtained to provide more physical insight about the system. In addition, the results unveil the significant effect of the system and channel parameters on proposed system. The results show that the system with RIS offers better performance compared the system without RIS. The analytical results are verified by Monte-Carlo simulation to justify the accuracy of the derived expressions.

INDEX TERMS Reconfigurable intelligent surface, high altitude platform station, amplify-and-forward relaying, outage probability, average bit error rate, average capacity.

I. INTRODUCTION

Recently, the applications of high-altitude platform stations (HAPSs) have gained tremendous interest in the research community as a new solution to realize communication between two ground stations [1]. They have been explored to play an important role in deploying of emergency communication supporting services during large scale disaster monitoring. Owing to communication challenges as a result of geographical complexity of the disaster area, HAPS has been considered to be suitable in establishing communication for both the rescue team and survivors [2]. In addition to this application, it has been suggested to offer an effective solution to ever increasing in cost of infrastructure deployment by providing network for incumbent and new entrant network operators at lower cost [3]. As a flying platform, HAPS is usually positioned in the stratosphere zone at altitude between 17 to 22 *km* above the earth surface [4]. It has features of both terrestrial and satellite communications and thus utilizes the advantages of both the communication systems [5]. In this case, a large footprint of 100 *km* radius has been suggested by International Telecommunication Union (ITU) to act as HAPS [3]. In most literature, HAPSs have been considered as relaying assisting node in different configurations such as HAPS-to-HAPS [6], Ground-to-HAPS [7] and Satellite-to-HAPS [8]–[11]. In [6], performance of a HAPS-based multi-hop relaying free space optical (FSO) communication using all-optical relaying and coherent receiver was evaluated. The performance analysis of HAPS-based relaying FSO was studied in [7] where

The associate editor coordinating the review of this manuscript and approving it for publication was Anandakumar Haldorai.

spatial diversity was considered for the system. Also, the performance of hybrid radio frequency (RF)/FSO HAPS-based relaying network for downlink satellite communication was presented in [8]. In [9], the performance of HAPS-based relaying for integrated space-air-ground network with hybrid RF/FSO communication is evaluated. Moreover, HAPS selection for hybrid RF/FSO communication system was proposed in [11], where the satellite selects the HAPS with the highest SNR. Yahia *et al.* [10] studied the performance of HAPS to increase the performance of satellite networks.

Reconfigurable intelligent surface (RIS) has been considered as an innovative technology of assisting the wireless communication systems from transmission blockage without sending any information of its own. The RISs are made up of planner metal surface that consist of larger number of low-cost configurable passive elements [12]. Artificially, it controls the characteristic of the incident signal such as phase, amplitude and polarization via integrated electronic towards a desire direction [13], [14]. It enhances the quality of the received signal by increasing the number of reflecting elements [15]. Compared with active relaying counterpart, it requires no additional power and complex processing operations for signal transmission, amplification, and regeneration to achieve high spectrum efficiency [16]. Therefore, this make RISs easy to be integrated into the current wireless communication systems without any changes in hardware [15]. In addition, the research has shown that RISs offer better performance than traditional multiple AF relaying systems and massive multiple input and multiple output networks, while reducing the system complexity and cost [17]. Due to these excellent features, RISs have been envisaged to play a key role in future communication systems. In [18], the performance of RIS-assisted power line communication network under different relay protocol was evaluated. Also, the performance analysis of an RIS-assisted non-orthogonal multiple access network was presented in [19]. The authors in [20] studied the performance of a RIS-assisted mobile network with random mobile users. Moreover, the performance analysis of RIS in a dual-hop decode-and-forward (DF) relay empowered mixed RF/FSO was presented in [21] where RIS was used to enhance both the RF and FSO links. Odeyemi *et al.* [22], investigated the performance of RIS in a wireless powered interference limited communication network. Also, the impact of interference on the DF relay network with the RIS-assisted source and relay was investigated in [17]. In [23], [24], the authors studied the physical layer security performance in vehicular networks with different modes of RIS. Furthermore, the authors in [25] studied the performance RIS-aided underwater communication system. The performance of RIS in the mixed RF/FSO dual-hop system was presented in [26] where the authors considered opportunistic users scheduling. In addition, performance of RIS-empowered UAV relaying network was investigated in [27].

In all the aforementioned research studies above, the HAPS and RIS were proposed to revolutionize the well explored existing active relaying networks. However, the performance of RIS in HAPS relaying network still remain at infancy stage. Motivated by this, the performance RIS-assisted HAPS relaying communication network for multiple ground users is presented in this paper. In this network, the RIS is used to reflect the source signal from the ground to the HAPS and the HAPS utilized semi-blind fixed AF relaying protocol to transmit the source signal to the multiple users at the destination. Therefore, the CDF and PDF of the system equivalent end-to-end SNR are derived by exploring Meijer's G and Fox's H functions. Through these expressions, the exact closed-form expressions for system outage probability, average BER and average capacity are obtained. In addition, the system asymptotic expression is derived in order to gain useful performance insight about the concerned system. Thus, the main contributions of this study are summarized as follows:

i. The CDF and PDF of the system equivalent end-to-end SNR are derived by exploring Meijer's G and Fox's H functions.
ii. The performance metrics in terms of outage probability, average BER and average capacity are obtained for the concerned system.
iii. The asymptotic expression for the system outage probability is derived.
iv. Relative to [27] where the RIS assisted an unmanned aerial vehicle (UAV) relaying node, the UAV employed DF relay protocol for signal transmission and the system considered a single user at the destination. In this paper, however, an AF relaying protocol is proposed for the HAPS and the system consider multiple users at the destination.

The rest of the paper is organized as follows. In Section II, the system and channel model and are provided. The system CDF and PDF exact analytical expressions of end-to-end SNR are derived in Section III. In Section IV, the system outage probability average BER and average capacity with asymptotic expression are presented. Numerical results and discussions are detailed in Section V and finally, concluding remarks are given in Section VI.

II. SYSTEM AND CHANNEL MODELS

The scenario depicted in Figure 1 in this paper illustrates an AF-based HAPS relaying node assisting the source in transmitting its information to the multiple users at the destination through a RIS with N_R reflecting elements. It is assumed that there is transmission blockage between the source and the users as a result of natural obstacles such as high building or small hills. In this relaying network, the overall transmission occurs in two phases. During the first transmission phase, the source transmits its signal to the RIS which is reflected to the HAPS with optimal phase shift. In the second transmission phase, the HAPS utilizes AF

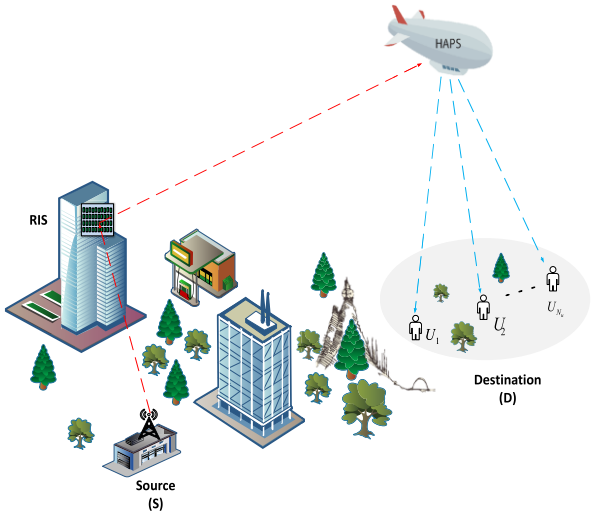

FIGURE 1. RIS-assisted AF-HAPS relaying communication network model.

relaying strategies to amplify the source signal and forward the amplified signal to the multiple users at the destination.

A. SOURCE-RIS-HAPS CHANNEL

The received signal at the HAPS can be expressed as:

$$y_1 = \left[\sum_{n=1}^{N} \alpha_n e^{j\phi_n} \beta_n\right] x_s + z_1. \tag{1}$$

where x_s is the information signal transmitted by the source, ϕ_n denotes the phase shift used by the $n-th$ reflecting element of the RIS, $\alpha_n = d_{SR}^{-\sigma/2} g_n exp^{-\psi_n}$ and $\beta_n = d_{RH}^{-\sigma/2} \upsilon_n exp^{-\vartheta_n}$ are the channel gain of RIS with g_n and υ_n are envelop of the α_n and β_n which are distributed as Rayleigh and Rician random variable respectively, d_{SH}^{σ} and d_{RH}^{σ} are the distance of Source-to-RIS and RIS-to-HAPS respectively, σ is the path-loss index, and z_1 signifies the additive white Gaussian noise (AWGN) with the noise power N_o.

According to [28], the maximum SNR can be achieved at HAPS by setting $\phi_n = \psi_n + \vartheta_n$ to eliminate the channel phases. Hence, the received SNR at the HAP can be further be simplified as:

$$y_1 = \sqrt{P_s}\left[\sum_{n=1}^{N} g_n \upsilon_n\right] x_s + z_1. \tag{2}$$

Therefore, from (2) the instantaneous SNR at HAPS can be expressed as:

$$\gamma_1 = \bar{\gamma}_1 P_s = \frac{\left(\sum_{n=1}^{N} g_n \upsilon_n\right)^2 P_s}{N_o \left(D_1\right)^{\sigma}}. \tag{3}$$

where $\bar{\gamma}_1$ is the average SNR at HAPS, P_s denotes the source transmit power and $D_1 = d_{SR} d_{RH}$

Thus, the probability density function (PDF) of the instantaneous SNR for the link follows the approximate generalized-K fading distribution and can be expressed as [29]:

$$f_{\gamma_1}(\gamma_1) = \frac{2\xi^{k_p+m_p} \gamma_1^{((k_p+m_p)/2-1)}}{\Gamma(k_p)\Gamma(m_p)(\bar{\gamma}_1/D_1)^{(k_p+m_p)/2}} \times K_{k_p-m_p}\left(2\xi\sqrt{\frac{\gamma_1 D_1}{\bar{\gamma}_1}}\right), \tag{4}$$

where k_p and m_p indicate the distribution parameters and $\xi = \sqrt{k_p m_p / \Omega_p}$ with the Ω_p signifies the mean power, $K_v(.)$ represents the modified Bessel function of the second kind with zero order and $\Gamma(.)$ is the Gamma function.

By converting the modified Bessel function in (4) to Meijer-G function using the identity stated in [30, Eq. (14)], the PDF of the instantaneous SNR of the link can be further expressed as:

$$f_{\gamma_1}(\gamma_1) = M\gamma_1^{\omega_1 - 1} G_{0,2}^{2,0}\left(\frac{\xi^2 D_1}{\bar{\gamma}_1}\gamma_1 \middle| \begin{matrix} - & , & - \\ \omega_2, & & -\omega_2 \end{matrix}\right). \tag{5}$$

where $M = \frac{\xi^{kp+mp}}{\Gamma(k_p)\Gamma(m_p)(\bar{\gamma}_1/D_1)^{\omega_1}}$, $\omega_1 = \left(k_p + m_p\right)/2$ and $\omega_2 = \left(k_p - m_p\right)/2$

Similarly, the CDF of the link instantaneous SNR can be obtained from (5) by applying the integral identity detailed in [30, Eq. (26)] as:

$$F_{\gamma_1}(\gamma_1) = M\gamma_1^{\omega_1} G_{1,3}^{2,1}\left(\frac{\xi^2 D_1}{\bar{\gamma}_1}\gamma_1 \middle| \begin{matrix} 1-\omega_1 \\ \omega_2, -\omega_1, -\omega_2 \end{matrix}\right). \tag{6}$$

B. HAPS RELAY-TO-USERS CHANNEL

At the destination D, the received signal at the $i-th$ users can be defined as:

$$y_{2,i} = G\sqrt{P_H} h_{u,i} y_1 + z_{u,i}, \tag{7}$$

where $G = \sqrt{\frac{1}{P_s\left|\sum_{n=1}^{N} g_n \upsilon_n\right|^2 + N_o}}$ denotes the amplifying factor, $h_{u,i}$ is the channel coefficient between HAPS to the $i-th$ user and $z_{u,i}$ represents the AWGN with the noise power N_o. Thus, the equivalent end-to-end instantaneous SNR at the $i-th$ users can then be expressed as:

$$\gamma_{eq,i} = \frac{\gamma_1 \gamma_{2,i}}{\gamma_{2,i} + C}, \tag{8}$$

where C signifies the fixed relay amplifying gain, $\gamma_{2,i} = \bar{\gamma}_2 \left|h_{u,i}\right|^2$ with $\bar{\gamma}_2 = P_H / N_o D_{2,i}^{\sigma}$ denotes the average SNR at the destination, $D_{2,i}$ indicate the distance between the HAPS and the $i-th$ user and P_H represents the HAPS transmit power. To harness the multiusers diversity, opportunistic user scheduling technique is adopted for the concerned system [31], wherein the HAPS selects the best user with the largest instantaneous SNR of the HAPS to $i-th$ link as:

$$\gamma_2 = \max_{1 \le i \le N} \gamma_{2,i} \tag{9}$$

Based on (9), the actual equivalent end-to-end SNR with the scheduled user under the AF relay protocol can thus be defined as:

$$\gamma_{eq} = \frac{\gamma_1 \gamma_2}{\gamma_2 + C}. \tag{10}$$

Moreover, it is assumed that the HAPS is located in space for wide coverage especially during disaster, then the HAPS-to-users link experience masking effect which can be characterized to follows Shadowed-Rician fading distribution and the PDF of instantaneous SNR γ_2 between the HAPS and the $i-th$ user can be expressed as [32]:

$$f_{\gamma_{2,i}}(\gamma_2) = \psi exp(-a\gamma_2)_1 F_1(m_h; 1; \delta\gamma_2), \tag{11}$$

where $\psi = 1/2\left(\frac{2bm_h}{2bm_h+\Omega}\right)^{m_h}$, $a = 1/2b$ and $\delta = \Omega/2b(2bm_h+\Omega)$ with Ω, m_h and $2b$ being the average power of LOS, fading severity parameter and the multipath component respectively.

$${}_1F_1(m_h; 1; \delta\gamma_2) = exp(\delta\gamma_2)\sum_{q=0}^{m_u-1}\frac{(1-m_u)_q(-\delta\gamma_{SR})^q}{(q!)^2} \tag{12}$$

where $(.)_q$ denotes the Pochhammer symbol

By invoking (12) into (11), the Shadowed-Rician distribution can be further simplified as:

$$f_{\gamma_{2,i}}(\gamma_2) = \sum_{q=0}^{m_u-1}\frac{\psi(1-m_u)_p(-\delta)^q}{(p!)^2(\bar{\gamma}_1)^{q+1}}\gamma_2^q\exp(-\lambda_H\gamma_2), \tag{13}$$

where $\lambda_H = D_{2,i}(a-\delta)/\bar{\gamma}_2$

By utilizing the opportunistic scheduling given in (9) and following the same approach given in [33], the Shadowed-Rician distribution PDF of the γ_2 for the link between the HAPS to the selected user is given as:

$$f_{\gamma_2}(\gamma_2) = \sum_{q_1=0}^{m_u-1}\cdots\sum_{q_{N_u}=0}^{m_u-1}\Psi(N_s)\gamma_2^{\eta-1}\exp(-\lambda_H\gamma_2), \tag{14}$$

where

$$\Psi(N_u) = \prod_{j=1}^{N_u}\rho(q_j)\alpha^{N_u}\prod_{\varepsilon=1}^{N_u-1}B\left(\sum_{k=1}^{\varepsilon}q_k+\varepsilon, q_{\varepsilon+1}+1\right), \tag{15a}$$

with $B(.,.)$ denotes Beta function

$$\rho(q_j) = \frac{(1-m_u)_{q_j}(-\delta)^{q_j}}{(q_j!)^2(\bar{\gamma}_2)^{q_j+1}}, \tag{15b}$$

$$\eta = \sum_{i=1}^{N_s}q_j + N_u. \tag{15c}$$

By integration (14) using the integral identity detailed in[34, Eq. (3.351(1))], the CDF of the link can be obtained as:

$$F_{\gamma_2}(\gamma_2) = \sum_{q_1=0}^{m_u-1}\cdots\sum_{q_{N_u}=0}^{m_u-1}\Psi(N_u)\lambda_H^{-\eta}\gamma(\eta, \lambda_R\gamma), \tag{16}$$

where $\gamma(.,.)$ is the lower incomplete Gamma function

By utilizing the [35, Eq. (8.4.16(1))] to represent the incomplete Gamma function in Meijer-G function form, then the (13) can be expressed as:

$$F_{\gamma_2}(\gamma) = \sum_{q_1=0}^{m_u-1}\cdots\sum_{q_{N_u}=0}^{m_u-1}\Psi(N_u)\lambda_H^{-\eta}G_{1,2}^{1,1}\left(\lambda_H\gamma\middle|\begin{matrix}1\\ \eta,\ 0\end{matrix}\right). \tag{17}$$

III. STATISTICS OF END-TO-END SNR

In this section, the exact closed-form expressions of CDF and PDF of the end-to-end instantaneous SNR of the proposed system are derived.

A. CUMULATIVE DISTRIBUTION FUNCTION

Following the same approach in [36], the CDF of the equivalent end-to-end SNR γ_{eq} can be expressed as:

$$F_{\gamma_{eq}}(\gamma) = F_{\gamma_1}(\gamma) + \underbrace{\int_0^{\infty}F_{\gamma_2}\left(\frac{C\gamma}{x}\right)f_{\gamma_1}(x+\gamma)dx}_{I_1}, \tag{18}$$

Theorem 1: The exact analytical CDF expression of the equivalent end-to-end SNR can be obtained in terms of the Meijer-G and Bivariate Fox's H-functions as:

$$\begin{aligned}F_{\gamma_{eq}}(\gamma) &= M\gamma^{\omega_1}G_{1,3}^{2,1}\left(\frac{\xi^2D_1}{\bar{\gamma}_1}\gamma\middle|\begin{matrix}1-\omega_1\\ \omega_2, -\omega_1, -\omega_2\end{matrix}\right)\\ &+M\sum_{q_1=0}^{m_u-1}\cdots\sum_{q_{N_u}=0}^{m_u-1}\Psi(N_u)\lambda_H^{-\eta}\gamma^{\omega_1}\\ &\times H_{1,0:3,1:2,1}^{0,1:1,2:0,2}\left(\begin{matrix}(1+w_1,1,-1)\\ -\\ (1-\eta,1)(0,1)(1,1)\\ (0,1)\\ (1-w_2,1)(1+w_2,1)\\ (w_1,1)\end{matrix}\middle|\frac{1}{\lambda_HC}, \frac{\bar{\gamma}_1}{\xi^2D_1\gamma}\right).\end{aligned} \tag{19}$$

where $G_{p,q}^{m,n}[.]$ and $H_{b,c:f,h:p,q}^{a,d:e,g:m,n}[.]$ are the Meijer-G and Bivariate Fox's H-functions respectively

Proof: Please see Appendix A

B. PROBABILITY DISTRIBUTION FUNCTION

The PDF of the end-to-end instantaneous SNR can be determined by taking the derivative of (19) with respect to γ as:

$$f_{eq}(\gamma) = \frac{dF_{eq}(\gamma)}{d\gamma}, \tag{20}$$

Theorem 2: The exact analytical PDF expression of the equivalent end-to-end SNR can be obtained in terms of the

Meijer-G and Bivariate Fox's H-functions as:

$$f_{eq}(\gamma) = M\gamma^{\omega_1-1}G_{0,2}^{2,0}\left(\frac{\xi^2 D_1}{\bar{\gamma}_1}\gamma\middle|\begin{matrix}-, , -\\ \omega_2, -\omega_2\end{matrix}\right) + M\sum_{q_1=0}^{m_u-1}\cdots\sum_{q_{N_u}=0}^{m_u-1}\Psi(N_u)\lambda_H^{-\eta}\gamma^{\omega_1-1} \times H_{1,0:3,1:2,1}^{0,1:1,2:0,2}\left(\begin{matrix}(1+w_1,1,-1)\\ -\\ (1-\eta,1)(0,1)(1,1)\\ (0,1)\\ (1-w_2,1)(1+w_2,1)\\ (1+w_1,1)\end{matrix}\middle|\frac{1}{\lambda_H C},\frac{\bar{\gamma}_1}{\xi^2 D_1\gamma}\right). \quad (21)$$

Proof: Please see Appendix B

IV. PERFORMANCE ANALYSIS

In this section, the exact closed-form expressions of the system outage probability, average bit error rate (BER) and average capacity are derived. In addition, to obtain the useful performance insight about the proposed system, the asymptotic expressions of the system at high SNR are provided.

A. OUTAGE PROBABILITY

1) EXACT ANALYSIS

This describes the probability that the instantaneous SNR of the system falls below a predetermined threshold γ_{th} and can be mathematically defined as [37]:

$$P_{out}(\gamma_{th}) = Pr[\gamma < \gamma_{th}] = F_{eq}(\gamma_{th}), \quad (22)$$

Theorem 3: the concerned system outage probability can be obtained by invoking (19) into (22) as follows:

$$P_{out}(\gamma_{th}) = M\gamma_{th}^{\omega_1}G_{1,3}^{2,1}\left(\frac{\xi^2 D_1}{\bar{\gamma}_1}\gamma_{th}\middle|\begin{matrix}1-\omega_1\\ \omega_2,-\omega_1,-\omega_2\end{matrix}\right) + M\sum_{q_1=0}^{m_u-1}\cdots\sum_{q_{N_u}=0}^{m_u-1}\Psi(N_u)\lambda_H^{-\eta}\gamma_{th}^{\omega_1} \times H_{1,0:3,1:2,1}^{0,1:1,2:0,2}\left(\begin{matrix}(1+w_1,1,-1)\\ -\\ (1-\eta,1)(0,1)(1,1)\\ (0,1)\\ (1-w_2,1)(1+w_2,1)\\ (w_1,1)\end{matrix}\middle|\frac{1}{\lambda_H C},\frac{\bar{\gamma}_1}{\xi^2 D_1\gamma_{th}}\right). \quad (23)$$

2) ASYMPTOTIC ANALYSIS

Owing to the complexity of the derived outage probability given in (23) in terms of Meijer-G and Fox's H-functions, only limited useful performance insights about the concerned system can be achieved. As a result of this, asymptotic expression of the system outage probability at high SNR can be obtained when $\bar{\gamma}_1 \to \infty$ and $\bar{\gamma}_2 \to \infty$.

Corollary 4: For the cases of $\bar{\gamma}_1 \to \infty$ and $\bar{\gamma}_2 \to \infty$, the asymptotic expression for the system outage probability can be given as:

$$P_{out}^{Asy}(\gamma) \underset{\bar{\gamma}_1,\bar{\gamma}_2\to\infty}{\approx} \frac{\Gamma(m_a-k_a)}{\Gamma(1+k_a)\Gamma(m_a)}\left(\frac{\xi^2 D_1}{\bar{\gamma}_1}\gamma_{th}\right)^{k_a} + M\sum_{q_1=0}^{m_u-1}\cdots\sum_{q_{N_u}=0}^{m_u-1}\Psi(N_u)\lambda_H^{-\eta}\left(\frac{\xi^2 D_1\gamma_{th}}{\bar{\gamma}_1}\right)^{-\omega_1} \times\left(\frac{\xi^2 D_1\lambda_H C}{\bar{\gamma}_1}\gamma_{th}\right)^{\eta} \times\frac{\Gamma(w_2+w_1-\eta)\Gamma(w_1-w_2-\eta)\Gamma(\eta)}{\Gamma(1+\eta)}. \quad (24)$$

Proof: Please see Appendix C.

B. AVERAGE BIT ERROR RATE

The average BER for the various modulation schemes can be expressed as [38]–[40]:

$$P_b = \frac{q^p}{2\Gamma(p)}\int_0^\infty exp(-q\gamma)\gamma^{p-1}F_{eq}(\gamma)\,d\gamma, \quad (25)$$

where p and q are the parameters that determine the type of modulation scheme. For instance, $\{p = 1/2, q = 1\}$ denotes binary phase shift keying (BPSK) and for others are summarized in [41, Table 1].

Theorem 5: The average BER for the concerned system under different modulation can be expressed as:

$$P_b = \frac{q^{-\omega_1}M}{2\Gamma(p)}G_{1,3}^{2,1}\left(\frac{\xi^2 L_R}{q\bar{\gamma}_1}\middle|\begin{matrix}1-p-\omega_1,1-\omega_1\\ \omega_2,-\omega_1,-\omega_2\end{matrix}\right) + \frac{q^{-\omega_1}M}{2\Gamma(p)}\sum_{q_1=0}^{m_u-1}\cdots\sum_{q_{N_u}=0}^{m_u-1}\Psi(N_u)\lambda_R^{-\eta} \times H_{1,0:3,1:2,2}^{0,1:1,2:1,2}\left(\begin{matrix}(1+w_1,1,-1)\\ -\\ (1-\eta,1)(0,1)(1,1)\\ (0,1)\\ (1-w_2,1)(1+w_2,1)\\ (p+w_1,1)(w_1,1)\end{matrix}\middle|\frac{1}{\lambda_R C},\frac{q\bar{\gamma}_1}{\xi^2 L_R\gamma}\right). \quad (26)$$

Proof: Please see Appendix D

C. AVERAGE CAPACITY

The average capacity of the concerned system can be expressed as [36], [42]:

$$\bar{C} = \frac{1}{2\ln(2)}ln(1+\gamma)f_{eq}(\gamma)\,d\gamma, \quad (27)$$

Theorem 6: By putting (21) into (27), the exact closed form expression of the system average capacity can be obtained as follow (28), shown at the bottom of the next page,

Proof: Please see Appendix E

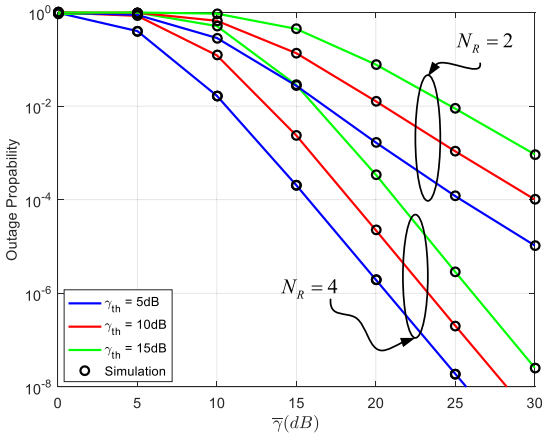

FIGURE 2. Outage performance of the system at different values of γ_{th} and N_R under FHS conditions.

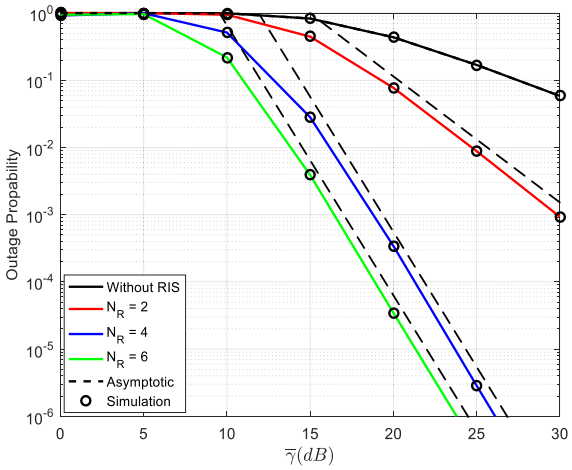

FIGURE 3. Effects of number of reflecting elements in RIS on the system outage performance.

V. NUMERICAL RESULTS AND DISCUSSION

In this section, the analytical and asymptotic results of the system outage probability, average BER and average capacity are provided to evaluate the influence of system and channel parameters on the concerned system performance. Monte-Carlo simulation is therefore employed to justify the accuracy of the derived expressions. For the HAPS-to-user link, the following shadowing severity parameters $(m = 1, b = 0.063, \Omega = 0.0007)$ and $(m = 5, b = 0.251, \Omega = 0.279)$ are defined for frequent heavy shadowing (FHS) and the average shadowing (AS) respectively [33]. With loss of generality, the $\bar{\gamma}_1 = \bar{\gamma}_2 = \bar{\gamma}$, $\gamma_{th} = 5dB$ $d_{SR} = d_{RH} = 2$ km, $D_2 = 4km$, $N_u = 2$ and $N_R = 2$. Under the system without RIS, it is assumed that the source equipped with single antenna communicates directly with the HAPS over Shadowing-Rician fading link.

The outage performance of the concerned system under different values of threshold SNR γ_{th} and number of reflecting elements N_R is presented in figure 2. The results show that the analytical results consistently matched with the simulation results. This observation justifies the accuracy of the derived exact outage probability expression. The results also indicate that the increase in γ_{th} significantly degrade the system outage performance. Also, it can be seen that the increase in N_R enhances the system performance with the large value of N_R offers the system better outage performance.

In figure 3, the impact of number of reflecting elements in RIS on the system outage performance is illustrated. According to the results, it can be depicted that asymptotic results approach the analytical results at high SNR. Also, the results indicate that as the number of reflecting elements in RIS increases, the better the quality of signal between the RIS and HAPS and this significantly enhances the system performance compared with the system without RIS.

The effect of Shadowing severity on the system performance under different users at the destination is demonstrated in figure 4. It can be observed that system performance is worsen under the FHS condition compared to AS condition. Also, the increase in the destination users improves the system diversity gain and hence offers better system outage performance.

The impact of HAPS distance from the destination users is presented in figure 5 under different Shadowing severity and the number of reflecting elements in RIS. It can be seen that the higher the HAPS distance from the users, the higher the system outage. Also, the system performance is worsened under the FHS conditions compared to AS condition. Under

$$\bar{C} = \frac{1}{2\ln(2)}\Bigg[MG_{24}^{4,1}\left(\frac{\xi^2 D_1}{\bar{\gamma}_1}\middle|\begin{matrix}-\omega_1, 1-\omega_1\\ \omega_2, -\omega_2, -\omega_1, -\omega_1\end{matrix}\right) + M\sum_{q_1=0}^{m_u-1}\cdots\sum_{q_{N_u}=0}^{m_u-1}\Psi\left(N_u\right)\lambda_H^{-\eta} \times H_{1,0:3,1:3,2}^{0,1:1,2:1,3}\left(\begin{matrix}(1+w_1,1,-1)\\ -\\ (1-\eta,1)\,(0,1)\,(1,1)\\ (0,1)\\ (1-w_2,1)\,(1+w_2,1)\,(1+w_1,1)\\ (1+w_1,1)\,(w_1,1)\end{matrix}\middle|\frac{1}{\lambda_H C},\frac{\bar{\gamma}_1}{\xi^2 D_1}\right). \tag{28}$$

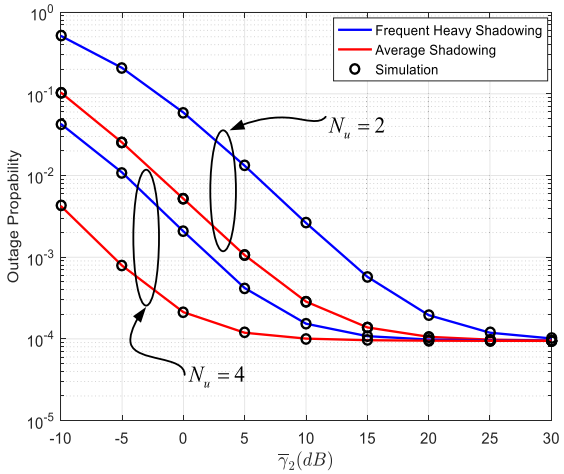

FIGURE 4. Impact of Shadowing Severity on the system performance at different number of destination users when $\bar{\gamma}_1 = 25dB$ and $\gamma_{th} = 5dB$.

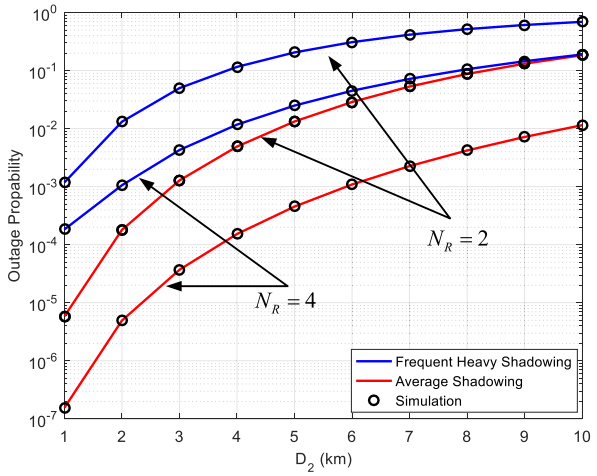

FIGURE 5. Impact of HAPS distance from the users under different Shadowing severities for different number reflecting elements in RIS.

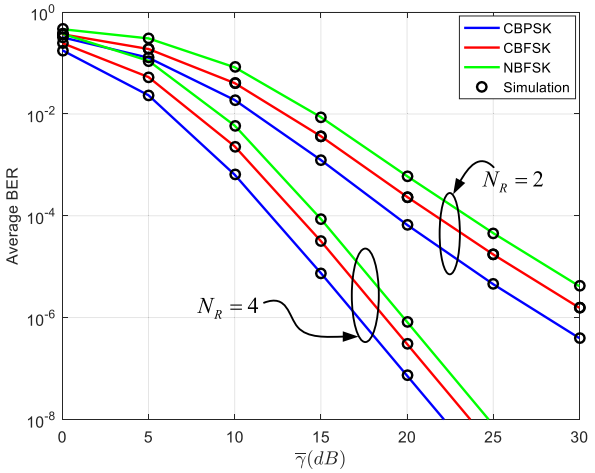

FIGURE 6. Error performance of the system under different modulation schemes and numbers of reflecting elements in RIS.

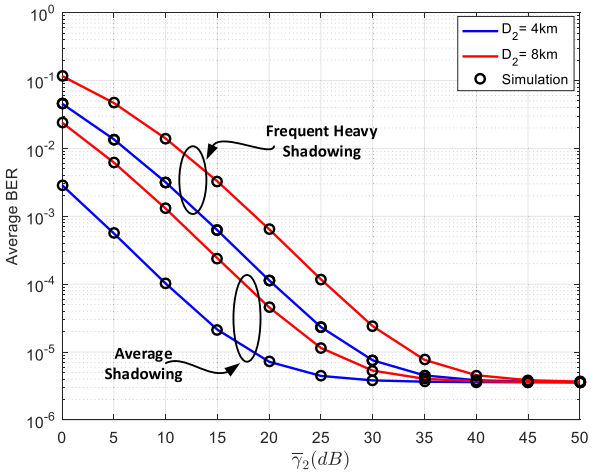

FIGURE 7. Impact of Shadowing severities and HAPS-to-users distance on the system error performance at $\bar{\gamma}_1 = 25dB$.

both conditions, however, the system outage performance is improved with the increase in the number of reflecting elements at the RIS with large values of N_R yields better performance.

The error performance of the system under different modulation schemes and number of reflecting elements in RIS is depicted in figure 6. Among the modulation schemes, it can be observed that CBPSK offers the system better performance. Also, the increase in the number of reflecting elements enhances the system error rate with high value of N_R yield better performance for all the modulation schemes. The results also indicate that the analytical results perfectly agreed with the simulation results which confirm the accuracy of the derived expressions.

In figure 7, the influence of Shadowing severity and HAP-to-user distance on the system error rate is presented. It can be observed that the error rate is better under the AS condition compared to FHS condition. The results also show that the increase in the HAPS distance from the users degrades the system error rate performance.

The error performance of the concerned system under different number of reflecting elements in RIS and number of destination users is illustrated in figure 8. The results show that the increase in the number of destination users the yields better system performance due to increase in system diversity gain. Also, the results indicate that there is noticeable decrease in system error rate as the number of reflecting elements in RIS increases compared with the system without RIS.

In figure 9, the system average capacity performance under the influence of the number of reflecting elements in RIS is presented. The results show that the increase in the number of reflecting elements in RIS offers the system better average capacity compared with system without RIS. It can also be observed that the analytical results perfectly matched with simulation results which prove the validity of the derived exact closed-form expression.

The influence of Shadowing severity on the system capacity performance under different users at the destination

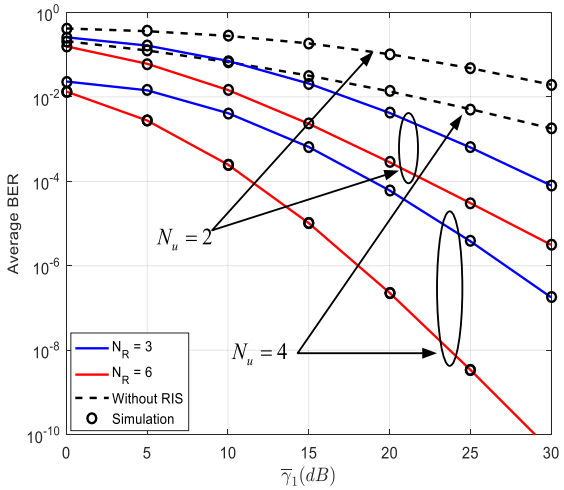

FIGURE 8. Error performance of the system under different number of users and reflecting elements in RIS at $\bar{\gamma}_2 = 10\,dB$.

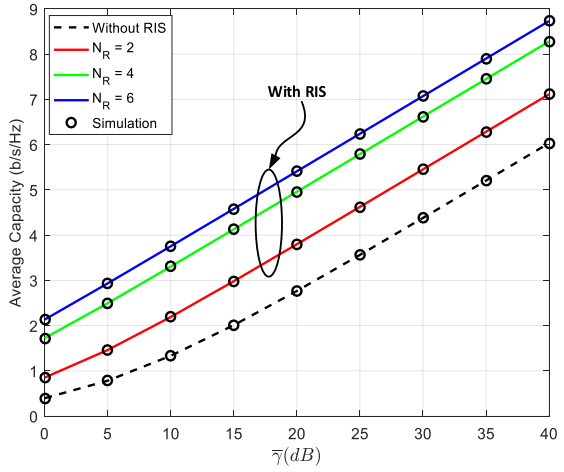

FIGURE 9. Impact of number of reflecting elements in RIS on the system capacity performance.

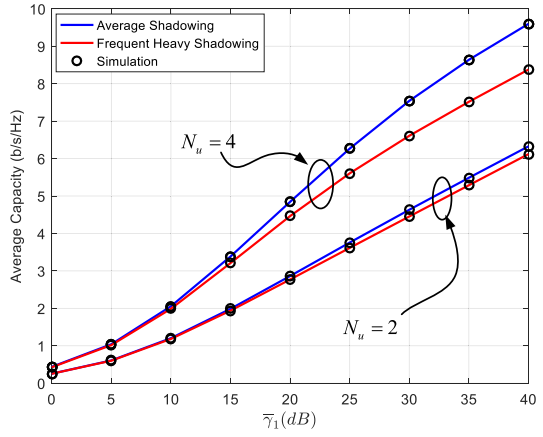

FIGURE 10. Capacity performance of the system under Shadowing severities and number of destination users at $\bar{\gamma}_2 = 5dB$.

is demonstrated in the figure 10. It can be clearly seen that the system capacity degrades under the FHS condition compared to AS condition. Under both conditions, the results show that the increase in the destination users enhances the system capacity performance due improvement in multiuser diversity gain.

VI. CONCLUSION

In this paper, the performance analysis of RIS-assisted AF-HAPS relaying communication network for multiple users is presented. The exact closed-form expressions for the system CDF and PDF of end-to-end instantaneous SNR are derived. Through these expressions, the system outage probability, average BER and average capacity are obtained in terms of the Meijer-G and Bivariate Fox's H-functions. Moreover, the asymptotic expression for the outage probability is determined in order to obtained more insight of the system performance. The results demonstrate the impact of number of RIS reflecting elements; Shadowing severity, number of destination users on the system preformation. In addition, the system with RIS outperform the system without RIS. The interesting future work could be focused on the non-orthogonal multiple access (NOMA) for better system spectrum efficiency.

.

APPENDIX A PROOF OF THEOREM 1

By substituting (5) and (17) into (18), the integral term of (16) can be expressed as:

$$I_1 = M \sum_{q_1=0}^{m_u-1} \cdots \sum_{q_{N_u}=0}^{m_u-1} \Psi(N_u) \lambda_H^{-\eta} \int_0^{\infty} G_{1,2}^{1,1}\left(\frac{\lambda_H C}{x}\gamma \middle| \begin{matrix} 1 \\ \eta, \quad 0 \end{matrix}\right) \times (x+\gamma)^{w_1-1} G_{0,2}^{2,0}\left(\frac{\xi^2 D_1}{\bar{\gamma}_1}(x+\gamma) \middle| \begin{matrix} - \\ \omega_2, -\omega_2 \end{matrix}\right) dx \tag{A.1}$$

By applying the [43, Eq. (1.112)], the Meijer-G function can be expressed in terms double integrals as follows:

$$\begin{aligned} I_1 = M & \sum_{q_1=0}^{m_u-1} \cdots \sum_{q_{N_u}=0}^{m_u-1} \frac{\Psi(N_u)\lambda_H^{-\eta}}{(2\pi i)^2} \\ & \times \int_{L_1}\int_{L_2} \frac{\Gamma(\eta+s_1)\Gamma(-s_1)}{\Gamma(1-s_1)} \Gamma(\omega_2+s_2) \\ & \times \Gamma(s_2-\omega_2)(\lambda_H C\gamma)^{-s_1} \times \left(\frac{\xi^2 D_1}{\bar{\gamma}_1}\right)^{-s_2} \\ & \times \int_0^{\infty} x^{s_1}(x+\gamma)^{w_1-s_2-1} dx ds_1 ds_2 \end{aligned} \tag{A.2}$$

where L_1 and L_2 denote for the contours in the s-plane and the t-plane, respectively.

By utilizing [34, Eq. (3.194(3)), Eq. (8.384(1))], the integral term of (A.2) can be solved as:

$$I_1 = M \sum_{q_1=0}^{m_u-1} \cdots \sum_{q_{N_u}=0}^{m_u-1} \frac{\Psi(N_u)\lambda_H^{-\eta}}{(2\pi i)^2} \gamma^{\omega_1} \times \int_{L_1}\int_{L_2} \Gamma(s_2-\omega_1+s_1) \frac{\Gamma(\eta+s_1)\Gamma(-s_1)\Gamma(s_1+1)}{\Gamma(1-s_1)} \times \frac{\Gamma(\omega_2+s_2)\Gamma(s_2-\omega_2)}{\Gamma(s_2-\omega_1+1)} (\lambda_R C)^{-s_1} \left(\frac{\xi^2 D_1 \gamma}{\bar{\gamma}_1}\right)^{-s_2} \times ds_1 ds_2 \quad (A.3)$$

By letting $s = s_1$ and $t = s_2$, then (A.3) can be rewritten as:

$$I_1 = M \sum_{q_1=0}^{m_u-1} \cdots \sum_{q_{N_u}=0}^{m_u-1} \frac{\Psi(N_u)\lambda_H^{-\eta}}{(2\pi i)^2} \gamma^{\omega_1} \times \int_{L_1}\int_{L_2} \Gamma(t-\omega_1-s) \frac{\Gamma(\eta+s)\Gamma(-s)\Gamma(s+1)}{\Gamma(1-s)} \times \frac{\Gamma(\omega_2+t)\Gamma(t-\omega_2)}{\Gamma(t-\omega_1+1)} (\lambda_H C)^{-s} \left(\frac{\xi^2 D_1 \gamma}{\bar{\gamma}_1}\right)^{-t} dsdt \quad (A.4)$$

By applying [44], the (A.4) can be expressed as:

$$I_1 = M \sum_{q_1=0}^{m_u-1} \cdots \sum_{q_{N_u}=0}^{m_u-1} \Psi(N_u)\lambda_H^{-\eta}\gamma^{\omega_1} \times H_{1,0:3,1:2,1}^{0,1:1,2:0,2}\left(\begin{matrix} (1+w_1,1,-1) \\ - \\ (1-\eta,1)(0,1)(1,1) \\ (0,1) \\ (1-w_2,1)(1+w_2,1) \\ (w_1,1) \end{matrix} \middle| \frac{1}{\lambda_H C}, \frac{\bar{\gamma}_1}{\xi^2 D_1 \gamma} \right) \quad (A.5)$$

By substituting (6) and (A.5) into (18), then the equivalent CDF in (19) is obtained

APPENDIX B PROOF OF THEOREM 2

Putting (19) into (20), the PDF can be expressed as:

$$f_{eq}(\gamma) = \frac{dQ_1}{d\gamma} + \frac{dQ_2}{d\gamma} \quad (B.1)$$

Then, the derivative of first term in (B.1) can be obtained as:

$$\frac{dQ_1}{d\gamma} = M\gamma^{\omega_1-1} G_{0,2}^{2,0}\left(\frac{\xi^2 L_R}{\bar{\gamma}_1}\gamma \middle| \begin{matrix} - & , & - \\ \omega_2, & & -\omega_2 \end{matrix}\right) \quad (B.2)$$

Similarly, from (20), Q_2 is defined as follows:

$$Q_2 = M \sum_{q_1=0}^{m_u-1} \cdots \sum_{q_{N_u}=0}^{m_u-1} \frac{\Psi(N_u)\lambda_H^{-\eta}}{(2\pi i)^2} \times \int_{L_1}\int_{L_2} \Gamma(t-\omega_1-s) \frac{\Gamma(\eta+s)\Gamma(-s)\Gamma(s+1)}{\Gamma(1-s)} \times \frac{\Gamma(\omega_2+t)\Gamma(t-\omega_2)}{\Gamma(t-\omega_1+1)} (\lambda_H C)^{-s} \left(\frac{\xi^2 D_1}{\bar{\gamma}_1}\right)^{-t} \times \frac{d\gamma^{\omega_1-t}}{d\gamma} dsdt \quad (B.3)$$

By using the identity $\Gamma(t-\omega_1+1) = (t-\omega_1)\Gamma(t-\omega_1)$, the (B.3) becomes:

$$Q_2 = M \sum_{q_1=0}^{m_u-1} \cdots \sum_{q_{N_u}=0}^{m_u-1} \frac{\Psi(N_u)\lambda_H^{-\eta}}{(2\pi i)^2} \gamma^{\omega_1-1} \times \int_{L_1}\int_{L_2} \Gamma(t-\omega_1-s) \frac{\Gamma(\eta+s)\Gamma(-s)\Gamma(s+1)}{\Gamma(1-s)} \times \frac{\Gamma(\omega_2+t)\Gamma(t-\omega_2)}{\Gamma(t-\omega_1)} (\lambda_H C)^{-s} \left(\frac{\xi^2 D_1 \gamma}{\bar{\gamma}_1}\right)^{-t} dsdt \quad (B.4)$$

By applying the identity detailed in [44], the derivative of second term of (B.1) can be solved as:

$$\frac{dQ_2}{d\gamma} = M \sum_{q_1=0}^{m_u-1} \cdots \sum_{q_{N_u}=0}^{m_u-1} \Psi(N_u)\lambda_H^{-\eta}\gamma^{\omega_1-1} \times H_{1,0:3,1:2,1}^{0,1:1,2:0,2}\left(\begin{matrix} (1+w_1,1,-1) \\ - \\ (1-\eta,1)(0,1)(1,1) \\ (0,1) \\ (1-w_2,1)(1+w_2,1) \\ (1+w_1,1) \end{matrix} \middle| \frac{1}{\lambda_H C}, \frac{\bar{\gamma}_1}{\xi^2 D_1 \gamma} \right) \quad (B.5)$$

By invoking (B.2) and (B.5) into (B.1), the PDF of the end-to-end instantaneous SNR in (21) is derived.

APPENDIX C PROOF OF THEOREM 3

To derive the asymptotic expression of outage probability, the asymptotic expressions of the first and the second term of (23) can be written as:

$$P_{out}^{Asy}(\gamma) \approx P_{Asy,1} + P_{Asy,2} \quad (C.1)$$

Assuming that $\bar{\gamma}_1 \to \infty$ and following the approach in [27], the first term of (23) can be expressed as:

$$P_{Asy,1} \underset{\bar{\gamma}_1 \to \infty}{\approx} \frac{\Gamma(m_a - k_a)}{\Gamma(1+k_a)\Gamma(m_a)} \left(\frac{\xi^2 D_1}{\bar{\gamma}_1}\gamma_{th}\right)^{k_a} \quad (C.2)$$

where $m_a = max(k_q, m_q)$ and $k_a = min(k_q, m_q)$

By using the identity defined [44], the second term of (23) can be expressed as:

$$P_{Asy,2} \underset{\bar{\gamma}_1\to\infty}{\approx} M \sum_{q_1=0}^{m_u-1} \cdots \sum_{q_{N_u}=0}^{m_u-1} \frac{\Psi(N_u)\,\lambda_H^{-\eta}}{(2\pi i)^2} \gamma^{\omega_1} \times \int_{L_1} \frac{\Gamma(\eta+s)\,\Gamma(-s)\,\Gamma(s+1)}{\Gamma(1-s)} (\lambda_H C)^{-s}\, ds \times \int_{L_2} \Gamma(t-\omega_1-s) \frac{\Gamma(\omega_2+t)\,\Gamma(t-\omega_2)}{\Gamma(t-\omega_1+1)} \left(\frac{\xi^2 D_1 \gamma_{th}}{\bar{\gamma}_1}\right)^{-t} dt \tag{C.3}$$

By applying the identity defined [43, Eq. (1.1)], the (C.3) can be simplified as:

$$P_{Asy,2} \underset{\bar{\gamma}_1\to\infty}{\approx} M \sum_{q_1=0}^{m_u-1} \cdots \sum_{q_{N_u}=0}^{m_u-1} \frac{\Psi(N_u)\,\lambda_H^{-\eta}}{2\pi i} \gamma^{\omega_1} \times \int_{L_1} \frac{\Gamma(\eta+s)\,\Gamma(-s)\,\Gamma(s+1)}{\Gamma(1-s)} (\lambda_R C)^{-s} \times H_{1,3}^{3,0}\left(\frac{\xi^2 D_1 \gamma_{th}}{\bar{\gamma}_1}\middle| \begin{matrix}(1-w_1,1)\\(-w_1-s,1)\,(w_2,1)\,(-w_2,1)\end{matrix}\right) ds) \tag{C.4}$$

Based on [45], when the argument tends to zero, the asymptotic value of the H-function can be defined as the residue of the closest pole to the left of the integration path l. Thus, by applying [46, Eq. (1.8.4)], the (C.4) can be expressed as:

$$P_{Asy,2} \underset{\bar{\gamma}_1\to\infty}{\approx} M \sum_{q_1=0}^{m_u-1} \cdots \sum_{q_{N_u}=0}^{m_u-1} \frac{\Psi(N_u)\,\lambda_H^{-\eta}}{2\pi i} \left(\frac{\xi^2 D_1 \gamma_{th}}{\bar{\gamma}_1}\right)^{-\omega_1} \times \int_{L_1} \frac{\Gamma(\eta+s)\,\Gamma(-s)\,\Gamma(s+1)}{\Gamma(1-s)} \times \frac{\Gamma(\omega_2+\omega_1+s)\,\Gamma(\omega_1-\omega_2+s)}{\Gamma(s+1)} \left(\frac{\xi^2 D_1 \lambda_H C}{\bar{\gamma}_1}\gamma_{th}\right)^{-s} ds \tag{C.5}$$

By using the integral identity detailed in [43, Eq. (1.1)], then (C.5) can be solved as:

$$P_{Asy,2} \underset{\bar{\gamma}_1\to\infty}{\approx} M \sum_{q_1=0}^{m_u-1} \cdots \sum_{q_{N_u}=0}^{m_u-1} \Psi(N_u)\,\lambda_H^{-\eta} \left(\frac{\xi^2 D_1}{\bar{\gamma}_1}\gamma_{th}\right)^{-\omega_1} \times H_{2,5}^{4,1}\left(\frac{\xi^2 D_1 \lambda_H C}{\bar{\gamma}_1}\gamma_{th}\middle| \begin{matrix}(1,1)\,(1,1)\\ \in_w\end{matrix}\right) \tag{C.6}$$

where $\in_w = (\eta,1)\,(1,1)\,(w_2+w_1,1)\,(w_1-w_2,1)\,(0,1)$

By invoking (C.2) and (C.6) into (C.1), then the asymptotic outage probability of the system at $\bar{\gamma}_1 \to \infty$ can be obtained as:

$$P_{out}^{Asy}(\gamma) \underset{\bar{\gamma}_1\to\infty}{\approx} \frac{\Gamma(m_a-k_a)}{\Gamma(1+k_a)\,\Gamma(m_a)} \left(\frac{\xi^2 D_1}{\bar{\gamma}_1}\gamma_{th}\right)^{k_a} + M \sum_{q_1=0}^{m_u-1} \cdots \sum_{q_{N_u}=0}^{m_u-1} \Psi(N_u)\,\lambda_H^{-\eta} \left(\frac{\xi^2 D_1 \gamma_{th}}{\bar{\gamma}_1}\right)^{-\omega_1} \times H_{2,5}^{4,1}\left(\frac{\xi^2 D_1 \lambda_H C}{\bar{\gamma}_1}\gamma\middle| \begin{matrix}(1,1)\,(1,1)\\ \in_w\end{matrix}\right) \tag{C.7}$$

Assuming that $\bar{\gamma}_2 \to \infty$, applying the identity in [46, Eq. (1.8.4)] to Fox's H-function in (C.7), then the asymptotic outage probability expression in (24) is obtained.

APPENDIX D PROOF OF THEOREM 4

Then, by substituting (19) into (25), the ABER of the system can be obtained as:

$$P_b = \frac{q^p}{2\Gamma(p)} [P_1 + P_2] \tag{D.1}$$

where the term P_1 can be expressed as:

$$P_1 = M \int_0^\infty \gamma^{p+\omega_1-1} \exp(-q\gamma) \times G_{1,3}^{2,1}\left(\frac{\xi^2 L_R}{\bar{\gamma}_1}\gamma\middle| \begin{matrix}1-\omega_1\\ \omega_2,-\omega_1,-\omega_2\end{matrix}\right) d\gamma \tag{D.2}$$

By applying the integral identity stated in [34, Eq. (8.813(1))], the (D.2) can be solved as:

$$P_1 = M q^{-p-\omega_1} G_{1,3}^{2,1}\left(\frac{\xi^2 L_R}{q\bar{\gamma}_1}\middle| \begin{matrix}1-p-\omega_1,1-\omega_1\\ \omega_2,-\omega_1,-\omega_2\end{matrix}\right) \tag{D.3}$$

Similarly, the second term of (D.1) can be expressed as:

$$P_2 = M \sum_{q_1=0}^{m_u-1} \cdots \sum_{q_{N_u}=0}^{m_u-1} \frac{\Psi(N_u)\,\lambda_R^{-\eta}}{(2\pi i)^2} \times \int_{L_1}\int_{L_2} \Gamma(t-\omega_1-s) \times \frac{\Gamma(\eta+s)\,\Gamma(-s)\,\Gamma(s+1)}{\Gamma(1-s)} \frac{\Gamma(\omega_2+t)\,\Gamma(t-\omega_2)}{\Gamma(t-\omega_1+1)} (\lambda_R C)^{-s} \times \left(\frac{\xi^2 L_R}{\bar{\gamma}_1}\right)^{-t} \int_0^\infty \gamma^{p+\omega_1-t-1} \times \exp(-q\gamma)\, d\gamma ds dt \tag{D.4}$$

By applying the integral identity detailed in [34, Eq. (3.326(2))], the (D.4) can be further expressed as:

$$P_2 = M \sum_{q_1=0}^{m_u-1} \cdots \sum_{q_{N_u}=0}^{m_u-1} \frac{\Psi\left(N_u\right)\lambda_R^{-\eta}}{q^{p+\omega_1}\left(2\pi i\right)^2} \times \int_{L_1}\int_{L_2} \Gamma\left(t-\omega_1-s\right) \times \frac{\Gamma\left(\eta+s\right)\Gamma\left(-s\right)\Gamma\left(s+1\right)}{\Gamma\left(1-s\right)} \times \frac{\Gamma\left(P+\omega_1-t\right)\Gamma\left(\omega_2+t\right)\Gamma\left(t-\omega_2\right)}{\Gamma\left(t-\omega_1+1\right)} \times \left(\lambda_R C\right)^{-s}\left(\frac{\xi^2 L_R}{q\bar{\gamma}_1}\right)^{-t} dsdt \tag{D.5}$$

By using the[44], the (D.5) can be solved as:

$$P_2 = M \sum_{q_1=0}^{m_u-1} \cdots \sum_{q_{N_u}=0}^{m_u-1} \frac{\Psi\left(N_u\right)\lambda_R^{-\eta}}{q^{p+\omega_1}} \times H_{1,0:3,1:2,1}^{0,1:1,2:0,2}\left(\begin{matrix}(1+w_1,1,-1)\\ -\\ (1-\eta,1)\,(0,1)\,(1,1)\\ (0,1)\\ (1-w_2,1)\,(1+w_2,1)\\ (p+w_1,1)\,(w_1,1)\end{matrix}\middle|\, \frac{1}{\lambda_R C}, \frac{q\bar{\gamma}_1}{\xi^2 L_R \gamma}\right) \tag{D.6}$$

By putting (D.3) and (D.6) into (D.1), the system average BER in (26) is obtained.

APPENDIX E PROOF OF THEOREM 5

By substituting (21) into (27), the system capacity can be expressed as:

$$\bar{C} = \frac{1}{2\ln(2)}\left[C_1 + C_2\right] \tag{E.1}$$

By converting $ln\left(1+\gamma\right)$ to Meijer-G function through the identity detailed in [30, Eq. (11)], the first term of (E.1) can be expressed as:

$$C_1 = M \int_0^\infty \gamma^{\omega_1-1} G_{2,2}^{1,2}\left(\gamma\middle|\begin{matrix}1,1\\1,0\end{matrix}\right) \times G_{0,2}^{2,0}\left(\frac{\xi^2 D_1}{\bar{\gamma}_1}\gamma\middle|\begin{matrix}-\\ \omega_2,-\omega_2\end{matrix}\right) d\gamma \tag{E.2}$$

By using the integral identity detailed in [30, Eq. (21)], the (E.2) can be expressed as:

$$C_1 = M G_{24}^{4,1}\left(\frac{\xi^2 D_1}{\bar{\gamma}_1}\middle|\begin{matrix}-\omega_1, 1-\omega_1\\ \omega_2, -\omega_2, -\omega_1, -\omega_1\end{matrix}\right) \tag{E.3}$$

Similarly, the second term of (E.1) can be expressed as:

$$C_2 = M \sum_{q_1=0}^{m_u-1} \cdots \sum_{q_{N_u}=0}^{m_u-1} \Psi\left(N_u\right)\lambda_H^{-\eta}\gamma^{\omega_1-1} G_{2,2}^{1,2}\left(\gamma\middle|\begin{matrix}1,1\\1,0\end{matrix}\right) \times H_{1,0:3,1:2,1}^{0,1:1,2:0,2}\left(\begin{matrix}(1+w_1,1,-1)\\ -\\ (1-\eta,1)\,(0,1)\,(1,1)\\ (0,1)\\ (1-w_2,1)\,(1+w_2,1)\\ (1+w_1,1)\end{matrix}\middle|\, \frac{1}{\lambda_H C}, \frac{\bar{\gamma}_1}{\xi^2 D_1 \gamma}\right) \tag{E.4}$$

By converting the Fox's H-function to integral form using the identity given in [44], then (E.4) can be further expressed as:

$$C_2 = M \sum_{q_1=0}^{m_u-1} \cdots \sum_{q_{N_u}=0}^{m_u-1} \frac{\Psi\left(N_u\right)\lambda_H^{-\eta}}{\left(2\pi i\right)^2} \times \int_{L_1}\int_{L_2} \Gamma\left(t-\omega_1-s\right)\frac{\Gamma\left(\eta+s\right)\Gamma\left(-s\right)\Gamma\left(s+1\right)}{\Gamma\left(1-s\right)} \times \frac{\Gamma\left(\omega_2+t\right)\Gamma\left(t-\omega_2\right)}{\Gamma\left(t-\omega_1\right)}\left(\lambda_H C\right)^{-s}\left(\frac{\xi^2 D_1}{\bar{\gamma}_1}\right)^{-t} \times \underbrace{\int_0^\infty \gamma^{\omega_1-t-1} G_{2,2}^{1,2}\left(\gamma\middle|\begin{matrix}1,1\\1,0\end{matrix}\right) d\gamma}\, dsdt \tag{E.5}$$

Using the integral identity detailed in [34, Eq. (7.811(4))], I_1 of (E.5) can be solved as:

$$I_1 = \frac{\Gamma\left(1+\omega_1-t\right)\Gamma\left(t-\omega_1\right)\Gamma\left(t-\omega_1\right)}{\Gamma\left(1-\omega_1+t\right)} \tag{E.6}$$

By invoking (E.6) into (E.5) and applying identity defined in[44], then (E.5) can be obtained as (E.7), shown at the bottom of the page. By substituting (E.3) and (E.7) into (E.1), the system average capacity in (28) is derived.

$$C_2 = M \sum_{q_1=0}^{m_u-1} \cdots \sum_{q_{N_u}=0}^{m_u-1} \Psi\left(N_u\right)\lambda_H^{-\eta} \times H_{1,0:3,1:3,2}^{0,1:1,2:1,3}\left(\begin{matrix}(1+w_1,1,-1)\\ -\\ (1-\eta,1)\,(0,1)\,(1,1)\\ (0,1)\\ (1-w_2,1)\,(1+w_2,1)\,(1+w_1,1)\\ (1+w_1,1)\,(w_1,1)\end{matrix}\middle|\, \frac{1}{\lambda_H C}, \frac{\bar{\gamma}_1}{\xi^2 D_1}\right) \tag{E.7}$$

REFERENCES

[1] S. Shah, M. Siddharth, N. Vishwakarma, R. Swaminathan, and A. S. Madhukumar, "Adaptive-Combining-Based hybrid FSO/RF satellite communication with and without HAPS," *IEEE Access*, vol. 9, pp. 81492–81511, 2021.

[2] L.-P. Zhu, X. Yan, and Y.-S. Zhu, "High altitude platform-based two-hop relaying emergency communications schemes," in *Proc. 5th Int. Conf. Wireless Commun., Netw. Mobile Comput.*, Sep. 2009, pp. 1–4.

[3] S. Kandeepan, T. Rasheed, and S. Reisenfeld, "Energy efficient cooperative HAP-terrestrial communication systems," in *Proc. Int. Conf. Pers. Satell. Services*. Berlin, Germany: Springer, 2011, pp. 151–164.

[4] M. Q. Vu, N. T. T. Nguyen, H. T. T. Pham, and N. T. Dang, "Performance enhancement of LEO-to-ground FSO systems using all-optical HAP-based relaying," *Phys. Commun.*, vol. 31, pp. 218–229, Dec. 2018.

[5] M. Sharma, D. Chadha, and V. Chandra, "High-altitude platform for free-space optical communication: Performance evaluation and reliability analysis," *J. Opt. Commun. Netw.*, vol. 8, no. 8, pp. 600–609, 2016.

[6] N. T. T. Nguyen, M. B. Vu, H. T. Le, V. V. Mai, and N. T. Dang, "HAP-based multi-hop FSO systems using all-optical relaying and coherent receiver," in *Proc. 6th NAFOSTED Conf. Inf. Comput. Sci. (NICS)*, Dec. 2019, pp. 119–124.

[7] N. T. T. Nguyen, M. Q. Vu, H. T. T. Pham, B. H. Dang, and T. D. Ngoc, "Performance enhancement of HAP-based relaying M-PPM FSO system using spatial diversity and heterodyne detection receiver," *J. Opt. Commun.*, vol. 42, no. 1, pp. 111–120, Jan. 2021.

[8] R. Swaminathan, S. Sharma, and A. S. MadhuKumar, "Performance analysis of HAPS-based relaying for hybrid FSO/RF downlink satellite communication," in *Proc. IEEE 91st Veh. Technol. Conf. (VTC-Spring)*, May 2020, pp. 1–5.

[9] S. R. S. Sharma, N. Vishwakarma, and A. S. Madhukumar, "HAPS-based relaying for integrated space–air–ground networks with hybrid FSO/RF communication: A performance analysis," *IEEE Trans. Aerosp. Electron. Syst.*, vol. 57, no. 3, pp. 1581–1599, Jun. 2021.

[10] O. Ben Yahia, E. Erdogan, and G. Karabulut Kurt, "On the use of HAPS to increase secrecy performance in satellite networks," 2021, *arXiv:2106.08180*.

[11] O. Ben Yahia, E. Erdogan, G. Karabulut Kurt, I. Altunbas, and H. Yanikomeroglu, "HAPS selection for hybrid RF/FSO satellite networks," 2021, *arXiv:2107.12638*.

[12] C. Huang, A. Zappone, G. C. Alexandropoulos, M. Debbah, and C. Yuen, "Reconfigurable intelligent surfaces for energy efficiency in wireless communication," *IEEE Trans. Wireless Commun.*, vol. 18, no. 8, pp. 4157–4170, Aug. 2019.

[13] A. R. Ndjiongue, T. M. N. Ngatched, O. A. Dobre, A. G. Armada, and H. Haas, "Analysis of RIS-based terrestrial-FSO link over G-G turbulence with distance and jitter ratios," *J. Lightw. Technol.*, vol. 39, no. 21, pp. 6746–6758, Nov. 1, 2021.

[14] D. Dixit, K. Chandra Joshi, and S. Sharma, "Performance of intelligent reconfigurable surface-based wireless communications using QAM signaling," 2020, *arXiv:2010.00519*.

[15] L. Yang, W. Guo, and I. S. Ansari, "Mixed dual-hop FSO-RF communication systems through reconfigurable intelligent surface," *IEEE Commun. Lett.*, vol. 24, no. 7, pp. 1558–1562, Jul. 2020.

[16] S. Basharat, S. A. Hassan, H. Pervaiz, A. Mahmood, Z. Ding, and M. Gidlund, "Reconfigurable intelligent surfaces: Potentials, applications, and challenges for 6G wireless networks," *IEEE Wireless Commun.*, vol. 28, no. 6, pp. 184–191, Dec. 2021.

[17] A. M. Salhab and L. Yang, "Interference impact on decode-and-forward relay networks with RIS-assisted source and relays," 2020, *arXiv:2011.05619*.

[18] K. O. Odeyemi, P. A. Owolawi, and O. O. Olakanmi, "On the performance of reconfigurable intelligent surface aided power line communication system under different relay transmission protocols," *Prog. Electromagn. Res. C.*, vol. 111, pp. 119–133, 2021.

[19] X. Yue and Y. Liu, "Performance analysis of intelligent reflecting surface assisted NOMA networks," *IEEE Trans. Wireless Commun.*, early access, Feb. 20, 2021, doi: 10.1109/TWC.2021.3114221.

[20] K. O. Odeyemi, P. A. Owolawi, and O. O. Olakanmi, "Reconfigurable intelligent surface assisted mobile network with randomly moving user over *Fisher-Snedecor* fading channel," *Phys. Commun.*, vol. 43, Dec. 2020, Art. no. 101186.

[21] K. O. Odeyemi, G. Aiyetoro, P. A. Owolawi, and O. O. Olakanmi, "Performance analysis of reconfigurable intelligent surface in a dual-hop DF relay empowered asymmetric RF/FSO networks," *Opt. Quantum Electron.*, vol. 53, no. 11, pp. 1–17, 2021.

[22] K. Odeyemi, P. Owolawi, and O. Olakanmi, "Reconfigurable intelligent surface in wireless-powered interference-limited communication networks," *Symmetry*, vol. 13, no. 6, p. 960, May 2021.

[23] A. U. Makarfi, K. M. Rabie, O. Kaiwartya, X. Li, and R. Kharel, "Physical layer security in vehicular networks with reconfigurable intelligent surfaces," in *Proc. IEEE 91st Veh. Technol. Conf. (VTC-Spring)*, May 2020, pp. 1–6.

[24] Y. Ai, F. A. P. de Figueiredo, L. Kong, M. Cheffena, S. Chatzinotas, and B. Ottersten, "Secure vehicular communications through reconfigurable intelligent surfaces," *IEEE Trans. Veh. Technol.*, vol. 70, no. 7, pp. 7272–7276, Jul. 2021.

[25] K. O. Odeyemi, P. A. Owolawi, and O. O. Olakanmi, "Performance analysis of reconfigurable intelligent surface assisted underwater optical communication system," *Prog. Electromagn. Res. M*, vol. 98, pp. 101–111, Nov. 2020.

[26] A. M. Salhab and L. Yang, "Performance analysis of RIS-assisted source mixed RF/FSO relay networks," 2020, *arXiv:2011.05612*.

[27] L. Yang, F. Meng, J. Zhang, M. O. Hasna, and M. D. Renzo, "On the performance of RIS-assisted dual-hop UAV communication systems," *IEEE Trans. Veh. Technol.*, vol. 69, no. 9, pp. 10385–10390, Sep. 2020.

[28] E. Basar, M. Di Renzo, J. De Rosny, M. Debbah, M. Alouini, and R. Zhang, "Wireless communications through reconfigurable intelligent surfaces," *IEEE Access*, vol. 7, pp. 116753–116773, 2019.

[29] L. Yang, F. Meng, Q. Wu, D. B. da Costa, and M.-S. Alouini, "Accurate closed-form approximations to channel distributions of RIS-aided wireless systems," *IEEE Wireless Commun. Lett.*, vol. 9, no. 11, pp. 1985–1989, Nov. 2020.

[30] V. S. Adamchik and O. I. Marichev, "The algorithm for calculating integrals of hypergeometric type functions and its realization in REDUCE system," in *Proc. Int. Symp. Symbolic Algebr. Comput. (ISSAC)*, 1990, pp. 212–224.

[31] K. An, M. Lin, and T. Liang, "On the performance of multiuser hybrid satellite-terrestrial relay networks with opportunistic scheduling," *IEEE Commun. Lett.*, vol. 19, no. 10, pp. 1722–1725, Oct. 2015.

[32] R. Xu, D. Guo, B. Zhang, K. Guo, and C. Li, "Secrecy performance analysis for hybrid satellite terrestrial relay networks with multiple eavesdroppers," in *Proc. 28th Wireless Opt. Commun. Conf. (WOCC)*, May 2019, pp. 1–5.

[33] N. I. Miridakis, D. D. Vergados, and A. Michalas, "Dual-hop communication over a satellite relay and shadowed Rician channels," *IEEE Trans. Veh. Technol.*, vol. 64, no. 9, pp. 4031–4040, Sep. 2015.

[34] I. S. Gradshteyn and I. M. Ryzhik, *Table of Integrals, Series, and Products*. New York, NY, USA: Academic Press, 2014.

[35] A. P. Prudnikov, I. U. A. Brychkov, and O. I. Marichev, *Integrals and Series: Special Functions*. Boca Raton, FL, USA: CRC Press, 1986.

[36] S. Li, L. Yang, D. B. da Costa, and S. Yu, "Performance analysis of UAV-based mixed RF-UWOC transmission systems," *IEEE Trans. Commun.*, vol. 69, no. 8, pp. 5559–5572, Aug. 2021.

[37] Q. Sun, Z. Zhang, Y. Zhang, M. Lopez-Benitez, and J. Zhang, "Performance analysis of dual-hop wireless systems over mixed FSO/RF fading channel," *IEEE Access*, vol. 9, pp. 85529–85542, 2021.

[38] E. Zedini, H. Soury, and M.-S. Alouini, "On the performance analysis of dual-hop mixed FSO/RF systems," *IEEE Trans. Wireless Commun.*, vol. 15, no. 5, pp. 3679–3689, May 2016.

[39] S. Li and L. Yang, "Performance analysis of dual-hop THz transmission systems over α-μ fading channels with pointing errors," 2021, *arXiv:13166*.

[40] D. Selimis, K. P. Peppas, G. C. Alexandropoulos, and F. I. Lazarakis, "On the performance analysis of RIS-empowered communications over Nakagami-m fading," *IEEE Commun. Lett.*, vol. 25, no. 7, pp. 2191–2195, Jul. 2021.

[41] S. Anees and M. R. Bhatnagar, "Performance of an amplify-and-forward dual-hop asymmetric RF-FSO communication system," *J. Opt. Commun. Netw.*, vol. 7, no. 2, pp. 124–135, 2015.

[42] P. Kumar Singya and M.-S. Alouini, "Performance of UAV assisted multiuser terrestrial-satellite communication system over mixed FSO/RF channels," 2021, *arXiv:2109.05762*.

[43] A. M. Mathai, R. K. Saxena, and H. J. Haubold, *The H-Function: Theory and Applications*. New York, NY, USA: Springer, 2009.
[44] P. Mittal and K. Gupta, "An integral involving generalized function of two variables," in *Proc. Indian Acad. Sci.-Sect. A*. Bengaluru, India: Springer, vol. 1972, vol. 75, no. 3, pp. 117–123.
[45] H. R. Alhennawi, M. M. El Ayadi, M. H. Ismail, and H.-A. M. Mourad, "Closed-form exact and asymptotic expressions for the symbol error rate and capacity of the H-function fading channel," *IEEE Trans. Veh. Technol.*, vol. 65, no. 4, pp. 1957–1974, Apr. 2015.
[46] A. A. Kilbas, *H-Transforms: Theory and Applications*. Boca Raton, FL, USA: CRC Press, 2004.

KEHINDE OLUWASESAN ODEYEMI received the B.Tech. degree in electronic engineering from the Ladoke Akintola University of Technology, Ogbomosho, Oyo State, Nigeria, in 2008, the M.Eng. degree in electronic engineering from the Federal University of Technology, Akure, in 2012, and the Ph.D. degree in electronic engineering from the University of KwaZulu-Natal, Durban, South Africa, in 2018. In 2019, he joined as a Research Fellow at the Innovative Research Group, Department of Computer Systems Engineering, Tshwane University of Technology, Pretoria, South Africa. He is currently a Senior Lecturer at the Department of Electrical and Electronic Engineering, University of Ibadan, Nigeria. He has written several research articles and his research interests include antenna design, optical wireless communications, reconfigurable intelligent surface, and cognitive radio systems. He is a member of the Council for the Regulation of Engineering in Nigeria (COREN).

PIUS ADEWALE OWOLAWI (Member, IEEE) received the B.Tech. degree in physics/electronics from the Federal University of Technology, Akure, in 2001, and the M.Sc. and Ph.D. degrees in electronic engineering from the University of KwaZulu-Natal, in 2006 and 2010, respectively. In 2007, he joined the Faculty of the Engineering, Department of Electrical Engineering, Mangosuthu University of Technology, South Africa. Thereafter, in 2017, he joined the Department of Computer Systems Engineering, Tshwane University of Technology, Pretoria, South Africa, where he is currently the Acting Head of Department. He has written several research articles. His research interests include computational of electromagnetic, modeling of radio wave propagation at high frequency, fiber optic communication, radio planning and optimization techniques, and renewable energy. He serves as a reviewer for many scientific journals. He is a member of several professional bodies, like SAIEE and SA AMSAT. He holds several industry certifications, such as CCNA, CCNP, CWNP, CFOA, CFOS/D, and MCITP.

OLADAYO OLUFEMI OLAKANMI received the B.Tech. degree in computer engineering from the Ladoke Akintola University of Technology, Nigeria, in 2001, and the M.Sc. degree in computer science and the Ph.D. degree in electrical and electronic engineering from the University of Ibadan, Nigeria, in 2006 and 2014, respectively. He is currently a Senior Lecturer with the Department of Electrical and Electronic Engineering, University of Ibadan. He is a Research Fellow at the Massachusetts Institute of Technology, USA. His research interests include security and privacy and embedded systems.